

Mechanism behind self-sustained oscillations in direct current glow discharges and dusty plasmas

Sung Nae Cho*

Devices R&D Center, Samsung Advanced Institute of Technology,
Samsung Electronics Co., Ltd, Mt. 14-1 Nongseo-dong,
Giheung-gu, Yongin-si, Gyeonggi-do 446-712, Republic of Korea.

(Dated: 2 April 2013)

An alternative explanation to the mechanism behind self-sustained oscillations of ions in direct current (DC) glow discharges is provided. Such description is distinguished from the one provided by the fluid models, where oscillations are attributed to the positive feedback mechanism associated with photoionization of particles and photoemission of electrons from the cathode. Here, oscillations arise as consequence of interaction between an ion and the surface charges induced by it at the bounding electrodes. Such mechanism provides an elegant explanation to why self-sustained oscillations occur only in the negative resistance region of the voltage-current characteristic curve in the DC glow discharges. Furthermore, this alternative description provides an elegant explanation to the formation of plasma fireballs in the laboratory plasma. It has been found that oscillation frequencies increase with ion's surface charge density, but at the rate which is significantly slower than it does with the electric field. The presented mechanism also describes self-sustained oscillations of ions in dusty plasmas, which demonstrates that self-sustained oscillations in dusty plasmas and DC glow discharges involve common physical processes.

I. INTRODUCTION

When an ion is confined between the two plane-parallel electrodes and is subject to static electric field (see Fig. 1), it begins to self-oscillate without damping. Such phenomenon is referred to as self-sustained oscillations in direct current (DC) glow discharges; and, it has been known for almost a century.¹⁻⁷ In literature, the phenomenon of DC glow discharge is also referred to as the DC glow corona. The mechanism behind such oscillations is still not fully understood.^{8,9,11-17} Over the years, various theoretical models have been proposed in an attempt to explain the phenomenon.^{5,11,18-26} Among the successful ones are those based on the fluid and equivalent circuit models.

The equivalent circuit models try to predict oscillations by representing the system with an equivalent RLC circuit, where R is a resistor, L is an inductor, and C is a capacitor.¹⁸⁻²¹ Although this approach is quite useful in describing oscillation frequencies as function of DC bias voltages, it says nothing about the mechanism behind self-sustained oscillations.

The fluid models approach the problem from more fundamental grounds of the electromagnetic theory. In this approach, the Poisson equation is solved in combination with the electron and the ion flux continuity equations, which constitute the so called positive feedback mechanism.²²⁻²⁶ Assertion of such feedback mechanism is crucial in the fluid models because, without it, no oscillatory solutions can be obtained. Typical sources of the positive feedback mechanism include the photoionization of particles and photoemission of electrons from the cathode. Physically, such feedback mechanism promotes oscillations by periodically reversing the particle's charge polarity. An ion oscillating near an electrode induces current in the same electrode, where the waveform of such current is correlated to its velocity profile.²³ Experimentally, it is this induced electrode current (or voltage) which gets measured.^{6,11} The hallmark of the fluid models is their potential to reproduce experimental measurements to a reasonably

good accuracy. In principle, with an appropriate specification of the positive feedback mechanism, the level of accuracy presented by the fluid models can always be improved. The feedback mechanism varies among different authors; and, this has been a subject area of ongoing debate among different fluid model theorists.^{11,22-26}

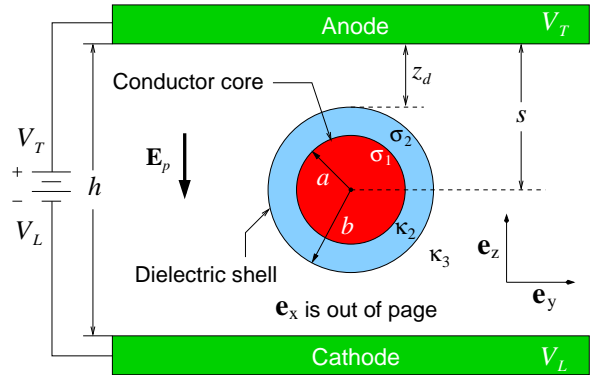


Figure 1: (Color online) Illustration of core-shell structured ion confined between DC voltage biased plane-parallel conductors with a vacuum gap of h . $\mathbf{E}_p = -\mathbf{e}_z(V_T - V_L)/h$ is the parallel plate electric field, where $(\mathbf{e}_x, \mathbf{e}_y, \mathbf{e}_z)$ are versors along the Cartesian (x, y, z) axes, respectively.

Does the aforementioned positive feedback mechanism, which is asserted in the fluid models, represent the fundamental mechanism behind the phenomenon of self-sustained oscillations in the DC glow discharges? This is a subtle question because I have shown recently that an ion confined between the DC voltage biased plane-parallel conductors goes through an undamped self-oscillatory motion.²⁷ Such self-oscillatory motion requires that an ion is electrically polarizable, but it does not necessarily involve or require the discussed positive feedback mechanism which is asserted in the fluid models. The fact that an ion must be electrically po-

larized excludes electrons from consideration in the discussion of self-oscillations presented in this work. However, the proton, which is known to be electrically polarizable,²⁸ is expected to self-oscillate in the DC glow discharges according to this alternative theory.

Remarkably, the predictions of this alternative theory²⁹ qualitatively agree with the predictions made by the fluid models.^{23,25} Both theories predict a saw-tooth shaped waveform for the induced currents in the electrodes. Furthermore, sharp pulses of radiation output are predicted by both theories to accompany the abrupt rises in the induced electrode currents. Such remarkable similarities in the predictions by the two very dissimilar theories suggest that the discussed positive feedback mechanism, which is asserted in the fluid models, may not necessarily represent the fundamental mechanism behind the phenomenon of self-sustained oscillations in the DC glow discharges.

In this work, I shall present some new aspects of this alternative theory²⁹ for further exploitation of the phenomenon of self-sustained ion oscillations in the DC glow discharges. These theoretical predictions are explicitly compared with various experimental results for the validation of the model. By direct application of the model to describe the charged-particle oscillations in dusty (or complex) plasmas experiments, I shall reveal that the phenomenon of self-sustained oscillations in both dusty plasmas and DC glow discharges involves a common physical mechanism in which self-oscillations are attributed to the interaction between an ionized particle and the surface charges induced by it at the surfaces of the particle confining electrodes. Considering that particle oscillations in both dusty plasmas and DC glow discharges experiments involve ionized particles that are only differ in their physical sizes and masses, such outcome is not too surprising. After all, apart from this, everything else is nearly identical from the physics point of view in both experiments.

II. BRIEF OUTLINE OF THE THEORY

The self-sustained oscillations in DC glow discharges are now discussed briefly in the framework of presented alterna-

tive theory using the configuration illustrated in Fig. 1. The electric potential between the plates is obtained by solving the Laplace equation with appropriate boundary conditions.²⁷ With this electric potential, induced surface charges at the surfaces of conductor plates are obtained by application of the Gauss's law. Such charge distributions act on an ion and generate resultant force given by $\mathbf{F}_T = \mathbf{F}_1 + \mathbf{F}_2 - \mathbf{e}_z mg$, where m is the mass of an ion, $g = 9.8 \text{ m/s}^2$ is the gravitational constant, and \mathbf{F}_1 (\mathbf{F}_2) is the force between the ion and the surface charges induced by it at the surface of anode (cathode). The explicit forms of \mathbf{F}_1 and \mathbf{F}_2 are given by²⁷

$$\mathbf{F}_1 = \mathbf{e}_z \pi \epsilon_0 \kappa_3 v \left\{ \frac{v}{4s^2} + E_p \left[\frac{\gamma(b^3 - a^3) - b^3}{4s^3} - 1 \right] \right\},$$

$$\mathbf{F}_2 = -\mathbf{e}_z \pi \epsilon_0 \kappa_3 v \left\{ \frac{v}{4(h-s)^2} - E_p \left[\frac{\gamma(b^3 - a^3) - b^3}{4(h-s)^3} - 1 \right] \right\},$$

where ϵ_0 is the vacuum permittivity, $E_p \equiv \|\mathbf{E}_p\|$ is the parallel-plate electric field strength, the parameter s is the distance from the ion's physical center to the anode; and, the terms γ and v are defined as

$$\gamma = \frac{3\kappa_3 b^3}{(\kappa_2 + 2\kappa_3)b^3 + 2(\kappa_2 - \kappa_3)a^3}, \quad (1)$$

$$v = \frac{2a(b-a)\sigma_1}{\epsilon_0 \kappa_2} + \frac{a^2 \sigma_1 + b^2 \sigma_2}{\epsilon_0 \kappa_3}, \quad (2)$$

where σ_1 (σ_2) is the surface charge density at the ion's core (shell) of radius $r = a$ ($r = b$), and the dielectric constants κ_2 and κ_3 are depicted in Fig. 1. The resultant force on an ion is, hence, given by

$$\mathbf{F}_T(z_d) = \mathbf{e}_z \frac{\pi \epsilon_0 \kappa_3 v}{4} \left\{ \frac{v}{(z_d + b)^2} - \frac{v}{(h - z_d - b)^2} + E_p \left[\frac{\gamma(b^3 - a^3) - b^3}{(z_d + b)^3} + \frac{\gamma(b^3 - a^3) - b^3}{(h - z_d - b)^3} - 8 \right] \right\} - \mathbf{e}_z mg, \quad (3)$$

where $s = z_d + b$ in \mathbf{F}_1 and \mathbf{F}_2 (see Fig. 1). The potential energy associated with this force is given by²⁹

$$U(z_d) = \frac{\pi \epsilon_0 \kappa_3 v}{4} \left\{ \frac{v}{z_d + b} + \frac{v}{h - z_d - b} - \frac{4v}{h} + E_p \left[\frac{\gamma(b^3 - a^3) - b^3}{2(z_d + b)^2} - \frac{\gamma(b^3 - a^3) - b^3}{2(h - z_d - b)^2} + 8 \left(z_d + b - \frac{h}{2} \right) \right] \right\} + mg \left(z_d + b - \frac{h}{2} \right); \quad (4)$$

and, the equation of motion associated with this force, i.e., Eq. (3), can be expressed as

$$\frac{d^2 z_d}{dt^2} = \frac{\pi \epsilon_0 \kappa_3 v}{4m} \left\{ \frac{v}{(z_d + b)^2} - \frac{v}{(h - z_d - b)^2} + E_p \left[\frac{\gamma(b^3 - a^3) - b^3}{(z_d + b)^3} + \frac{\gamma(b^3 - a^3) - b^3}{(h - z_d - b)^3} - 8 \right] \right\} - g, \quad (5)$$

where γ and v are defined in Eqs. (1) and (2), respectively.^{27,29}

III. COMPARISON TO THE EXPERIMENTS

Gases under pressure in general, including noble gases, are composed of atomic clusters, a state of matter between molecules and solids, due to Van der Waals interaction.³⁰⁻³² In gaseous argon, each spherical atomic clusters of radius $r \approx 1$ nm contains roughly 135 argon atoms.³¹ Modeling particles in the gas as atomic clusters is important because gases are delivered to the laboratories in pressurized containers, in which environment individual particles in gas exist in the form of atomic clusters. That said, I shall explicitly work with an argon atomic cluster of radius $r \approx 1$ nm, which for brevity is simply referred to as “ion” hereafter. Such ion is not expected to be core-shell structured like the one depicted in Fig. 1. The shell portion of an ion can be eliminated by choosing $b = a$, $\kappa_2 = \infty$, and $\sigma_2 = 0 \text{ C/m}^2$. For a positive ion, its surface charge density is given by $\sigma_1 = Nq_e / (4\pi a^2)$, where N is the number of electrons removed from the particle and $q_e = 1.602 \times 10^{-19} \text{ C}$ is the fundamental charge magnitude. Without loss of generality, and for the purpose of clear illustration in this work, I shall choose $N = 250$ and $a = 1$ nm. This corresponds to the ion’s surface charge density of $\sigma_1 \approx 3.19 \text{ C/m}^2$. Assuming the mass of an argon atom is $6.63 \times 10^{-26} \text{ kg}$, a spherical atomic cluster composed of 135 argon atoms has a total mass of $m \approx 8.95 \times 10^{-24} \text{ kg}$, where the masses of missing N electrons have been neglected. Purely for convenience, I shall assume that the cathode is grounded and the space between the two conductor plates in Fig. 1 is a vacuum with a gap of $h = 100$ nm. The obtained parameter values are summarized here for reference:

$$\begin{cases} \kappa_2 = \infty, \kappa_3 = 1, h = 100 \text{ nm}, V_L = 0 \text{ V}, \\ \sigma_1 \approx 3.19 \text{ C/m}^2, \sigma_2 = 0 \text{ C/m}^2, \\ m \approx 8.95 \times 10^{-24} \text{ kg}, b = a = 1 \text{ nm}. \end{cases} \quad (6)$$

Illustrated in Fig. 2 is a plot of the potential energy well, where Eq. (4) has been plotted for $V_T = 100 \text{ V}$ using the parameters defined in Eq. (6). The width l_D of the potential energy well decreases with an increase in the electric field strength E_p . Such characteristic provides an elegant explanation to the experimental observations in which the oscillation frequencies increase with the applied electric field strength. Fox seems to be the first to discuss on such characteristic using a parabolic potential model.³

In the case of positive ions, the potential energy well gets formed in vicinity of the anode at the presence of applied static electric field. On the other hand, for the negative ions, the same electric field results in formation of the potential energy well in vicinity of the cathode. Such characteristic

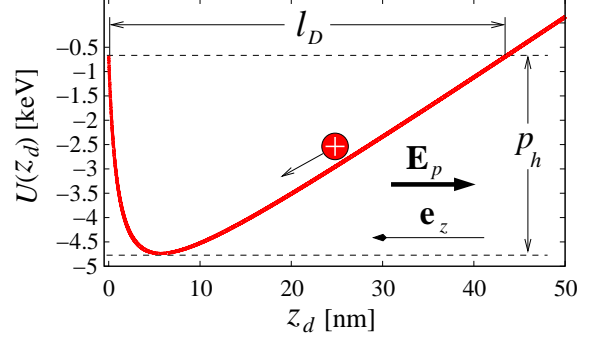


Figure 2: Potential energy is plotted for $V_T = 100 \text{ V}$ using parameter values defined in Eq. (6). Here, $V_T = 100 \text{ V}$ corresponds to $E_p = 1 \text{ GV/m}$.

provides an elegant explanation to the phenomenon of fireball formation in the laboratory plasma. When a positively biased electrode is immersed in plasma, a region of intense glow appears in vicinity of the electrode. Such glow formation is referred to as a plasma fireball.³³ In the framework of this alternative theory^{27,29} elaborated in this work, the formation of such plasma fireballs can be elegantly explained from the potential energy well which gets formed near the anode for positive ions. Since the dynamics of a plasma involves collective motions of its constituent atoms, a weakly ionized plasma fireball, as a whole, self-oscillates near the electrode as if it were a weakly ionized single superparticle. Throughout this work, I shall use the term “superparticle” to refer to such entity as plasma fireball whose dynamics can be represented by an equivalent single-particle picture. In the equivalent single-particle picture, the self-oscillation dynamics of a plasma fireball is described by the equation of motion defined in Eq. (5) with appropriate effective mass and surface charge densities prescribed. With that in mind, the plasma fireball effectively has a very large mass and carries a net charge which is very weak. Consequently, induced current oscillations of relatively low frequencies and small amplitudes are expected to be generated at the anode near a self-oscillating plasma fireball. Such prediction is consistent with the experimental observation by Stenzel *et al.*³³ Notice that this alternative theory can be directly applied to describe the self-oscillations of ionized dust particles in dusty plasmas. It is remarkable that the profile of the potential energy well illustrated in Fig. 2 qualitatively agrees with the measurements by Tomme *et al.*³⁴ and Arnas *et al.*³⁵ in dusty plasmas. Further discussion on this is provided in the sections A thru C of the appendix.

The particle’s equation of motion described in Eq. (5) can be solved via Runge-Kutta method using the parameter values

defined in Eq. (6) and the initial conditions given by

$$z_d(0) = 0.5 \text{ nm} \quad \text{and} \quad \frac{dz_d(0)}{dt} = 0 \frac{\text{nm}}{\text{s}}. \quad (7)$$

The results for $V_T = 50 \text{ V}$, 75 V , and 100 V are shown in Fig. 3(a), where it shows the oscillation frequencies increasing with the electric field strength. The oscillation frequencies also increase with the ion's surface charge density, but at the rate which is significantly slower than it does with the electric field strength (see Fig. 3(b)). For instance, when the electric field strength is doubled from $E_p = 0.5 \text{ GV/m}$ to $E_p = 1 \text{ GV/m}$, oscillation frequency nearly doubles from $\nu_{\text{osc}} \approx 104 \text{ GHz}$ to $\nu_{\text{osc}} \approx 191 \text{ GHz}$. However, doubling the ion's surface charge density, i.e., $\sigma_1 = Nq_e/(4\pi a^2)$, from $N = 250$ to $N = 500$ only slightly increases the oscillation frequency from $\nu_{\text{osc}} \approx 191 \text{ GHz}$ to $\nu_{\text{osc}} \approx 207 \text{ GHz}$. Such characteristics is consistent with the observations by Fox³ and Bořan *et al.*,³⁶ where they have reported that oscillation frequencies do not seem to be very dependent on the type of ions used in the discharge. It is well known that dissimilar atomic gases have different ionization tendencies. Based on this, it can be inferred that σ_1 , in general, for different atoms under identical conditions are different.

Although a relatively high static electric field is being applied to the ion in Fig. 3(a), its kinetic energies are small due to the fact that ion is going through frequent turnings inside a tight potential energy well. The ion's kinetic energy decreases with increased electric field strength for that matter and this is illustrated in Fig. 3(c). At the maximum speed of $\sim 2.912 \text{ km/s}$, the ion gains kinetic energy of $\mathcal{E}_K \approx 237 \text{ eV}$, which is small compared to the depth of $p_h \approx 4.1 \text{ keV}$ for the potential energy well but large compared to the average room temperature thermal energy of $\mathcal{E}_T = 1.5k_B T \approx 39 \text{ meV}$ (here, $T = 300 \text{ K}$ and $k_B = 8.62 \times 10^{-5} \text{ eV/K}$ is the Boltzmann constant). Self-sustained oscillations in the DC glow discharges can thus be expected to have high thermal stability.

In the experiments, self-sustained oscillations of ions in the DC glow discharges occur only in the negative resistance region of the voltage-current characteristic curve.^{12,14,18,24} Such negative resistance region in the voltage-current characteristic curve is characterized by $V_{\text{th1}} \leq V_T \leq V_{\text{th2}}$, where V_{th1} and V_{th2} are some threshold voltages. Equation (5) provides an elegant explanation to such properties. For instance, Eq. (5) yields solutions that are unphysical for $E_p < E_{p,\text{th1}}$ and $E_p > E_{p,\text{th2}}$, where $E_{p,\text{th1}}$ and $E_{p,\text{th2}}$ are the threshold electric field strengths. The physical solutions are only obtained for $E_{p,\text{th1}} \leq E_p \leq E_{p,\text{th2}}$. It is difficult to pinpoint $E_{p,\text{th1}}$ and $E_{p,\text{th2}}$ without the analytical solution of Eq. (5) at hand. Nevertheless, these can be roughly estimated on the grounds of physicality. To illustrate this, the oscillation frequency is first plotted as a function of the electric field strength in Fig. 3(d) by numerically solving Eq. (5) using the parameter values and the initial conditions from Eqs. (6) and (7), respectively. The solutions obtained for $E_p \lesssim 0.1 \text{ GV/m}$ and $E_p \gtrsim 4.9 \text{ GV/m}$ are unphysical. For instance, in the case of $E_p \gtrsim 4.9 \text{ GV/m}$, solutions show that the ion penetrates into the anode's surface whereas for $E_p \lesssim 0.1 \text{ GV/m}$, solutions yield peak to peak amplitudes that are larger than $h/2$. This latter case, although

mathematically allowed, is unphysical because, for a positive ion, oscillations can only exist for $z_d < h/2 - b$ from the argument based on the grounds of physicality.²⁷ Hence, the physical oscillatory solutions exist only for $0.1 \text{ GV/m} \lesssim E_p \lesssim 4.9 \text{ GV/m}$, where the upper and the lower bounds of E_p are only rough estimates based on the grounds of physicality arguments. Further discussion on the properties of the physical and the unphysical oscillatory solutions are provided in the section D of the appendix.

Recently, Lotze *et al.*³⁷ reported on an indirect account of oscillations involving a single H_2 molecule in the DC voltage biased conductors near an absolute zero temperature of $T = 5 \text{ K}$. According to their findings, the H_2 molecule in the junction, which is the space between the atomically clean $\text{Cu}(111)$ surface and the STM (scanning tunneling microscope) tip mounted on a cantilever, self-oscillates between the two unknown positional states when a threshold DC bias voltage is applied to the electrodes, i.e., the copper $\text{Cu}(111)$ surface and the STM tip. The footprint of self-sustained oscillations is the presence of the negative differential conductance in their measurement. Gupta *et al.*³⁸ showed that such negative differential conductance is due to the H_2 molecules in the junction. In the DC glow discharges, self-sustained oscillations arise as a consequence of the negative differential resistance.^{10,12,14} Since the negative differential conductance and the negative differential resistance are reciprocally related, they represent an equivalent description of the same physical processes. It is well known that the H_2 molecules can be ionized by a process of an electron impact.³⁹ When a threshold DC bias voltage is applied to the electrodes, the energetic electrons begin to tunnel through the junction. It is possible that the H_2 molecules in the junction are ionized in the process. If that is indeed the case, what Lotze *et al.* reported may be an indirect account of self-sustained oscillations involving a single or a few ions in the DC glow corona.²⁹ Their observation can serve as a catalyst for the future experiments in the few-particle DC plasma experiments.

Arnas *et al.*⁴⁰ reported that a dust particle made of hollow glass microsphere of radius $r \approx 32 \mu\text{m}$ with mass density of $\rho_m \approx 110 \text{ kg/m}^3$ and carrying a total electrical charge of $Q \approx -4.3 \times 10^5 q_e$, where $q_e = 1.602 \times 10^{-19} \text{ C}$, self-oscillates at a frequency of $\nu_{\text{osc}} \approx 17 \text{ Hz}$ inside the plasma sheath. The plasma sheath environment, in many respects, is similar to the empty space region between the DC voltage biased plane-parallel conductors. Ionized particle oscillations in the plasma sheath can therefore be modeled from the simple apparatus illustrated in Fig. 1. That said, the parameters and the initial conditions in the experiment by Arnas *et al.* can be summarized as follow:

$$\begin{cases} \kappa_2 = 6.5, \quad \kappa_3 = 1, \quad h = 5 \text{ mm}, \quad E_p = 5.15 \text{ kV/m}, \\ \sigma_1 = 0 \text{ C/m}^2, \quad \sigma_2 = -5.35 \mu\text{C/m}^2, \\ m \approx 15.1 \text{ ng}, \quad a = 0 \text{ m}, \quad b = 32 \mu\text{m}, \\ z_d(0) = 4.4 \text{ mm}, \quad \dot{z}_d(0) = 0 \text{ mm/s}, \quad \dot{z}_d \equiv dz_d/dt, \end{cases} \quad (8)$$

where the details of how these were obtained are explained in the section B of the appendix. Using these, the equation of motion described in Eq. (5) can be solved numerically via Runge-Kutta method. The result is shown in Fig. 4. One

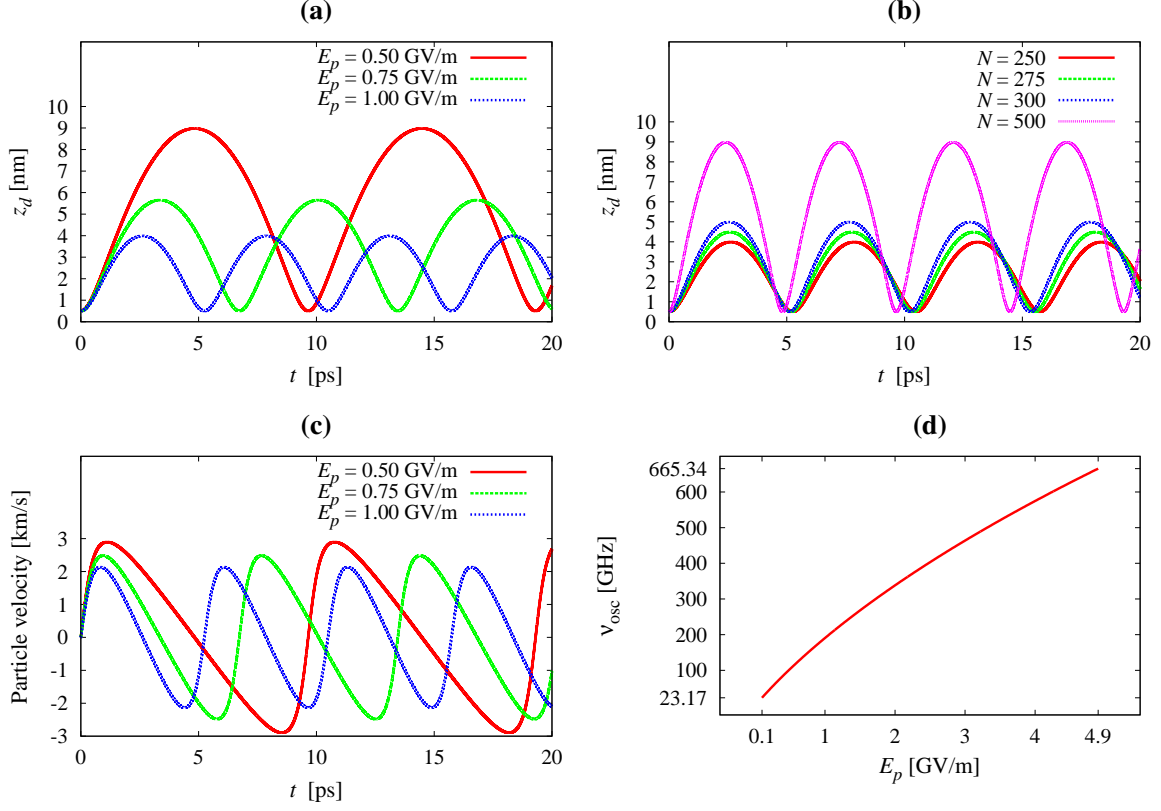


Figure 3: (Color online) Equation (5) is plotted, where in (a) electric field is varied and in (b) ion's surface charge density $\sigma_1 = Nq_e / (4\pi a^2)$ is varied at $E_p = 1 \text{ GV/m}$. (c) Ion velocity corresponding to the plot in (a). (d) Dependence of oscillation frequency v_{osc} on electric field strength E_p . Similar plot for the lower frequencies involving weakly charged ions subject to smaller E_p is also provided in the section E of appendix. In (a,b,c,d), all of the unspecified parameter values are from Eq. (6) and the initial conditions are from Eq. (7).

can readily verify that the particle oscillates at a frequency of approximately $v_{\text{osc}} \approx 17 \text{ Hz}$, which is consistent with the measurement by Arnas *et al.*⁴⁰

Although Arnas *et al.* explicitly states that their glass microsphere is hollow structured, their paper does not provide any information regarding the radius of the void inside of their hollow glass microsphere. Due to the lack of this information, the mass of an hollow glass microsphere in Eq. (8) has been computed assuming a solid microsphere. Such assumption overestimates the mass of an hollow glass microsphere. In fact, in their paper, Arnas *et al.* indicates the gravitational force of $F_g = (1.5 \pm 0.3) \times 10^{-10} \text{ N}$ for their hollow glass microsphere.⁴⁰ Such force corresponds to a mass of $m \approx 15.3 \text{ ng}$, which is exactly the mass computed assuming a solid glass microsphere in Eq. (8). If instead a smaller mass of $m \approx 6.19 \text{ ng}$ is assumed, an electric field strength of $E_p = 2.2 \text{ kV/m}$ is sufficient to generate an oscillation frequency of $v_{\text{osc}} \approx 17 \text{ Hz}$. This value for the electric field strength, i.e., $E_p = 2.2 \text{ kV/m}$, is consistent with the local electric field strength in the plasma sheath obtained by Arnas *et al.* in their dusty plasma experiment. The particle's oscillatory motion corresponding to this latter case, where $m \approx 15.1 \text{ ng}$ and $E_p = 5.15 \text{ kV/m}$, has been plotted in Fig. 4 for comparison.

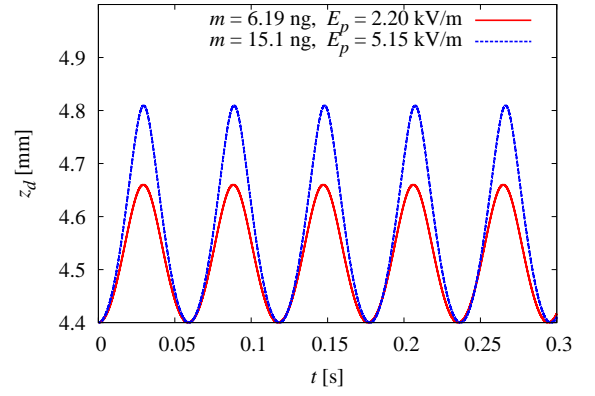


Figure 4: (Color online) Equation (5) is plotted using parameter values and initial conditions defined in Eqs. (8). Oscillation frequency of $v_{\text{osc}} \approx 17 \text{ Hz}$ is predicted by the theory, which is consistent with the measurement by Arnas *et al.*⁴⁰ In the plot, the anode is located at $z_d = 0 \text{ mm}$ and the cathode is located at $z_d = 5 \text{ mm}$.

This remarkable result demonstrates that self-sustained oscillations in both dusty plasmas and DC glow discharges share a common physical mechanism, in which the oscillations can

be attributed to the interaction between the ionized particle and the surface charges induced by it at the bounding electrodes. Such outcome makes sense because the oscillating ionized particles in both dusty plasmas and DC glow discharges experiments are only differ in their physical sizes and masses. Apart from this, the two systems are nearly identical in nature from the physics point of view.

Quite often in dusty plasmas, theoretical models based on simple harmonic excitations of small amplitude oscillations are employed for the description of the particle dynamics. One such model is given by⁴¹

$$\frac{d^2z}{dt^2} + v_{dn}\frac{dz}{dt} + \Omega_v^2 z = \frac{f_0 \cos \omega t}{m_d}, \quad (9)$$

where z is the particle displacement, m_d is the particle's mass, ω is the angular frequency of oscillation, t is the time, and f_0 is the amplitude of the external force. Particle's equation of motion based on such model, Eq. (9), is limited to the descriptions of oscillations involving a small amplitude displacements about the stationary equilibrium position. Besides this limitation, the equation of motion described by Eq. (9), as it stands, cannot be directly applied to describe the particle's oscillatory motion due to the fact that the quantities v_{dn} and Ω_v must be first determined experimentally.⁴² Consequently, Eq. (9) is only useful when determining the total charge carried by the particle. Although Eq. (9) provides an indirect method of measuring the particle's total charge, as it stands, it says nothing about the fundamental mechanism behind the self-sustained oscillations of ions in dusty plasmas.

The equation of motion described in Eq. (5) is distinguished from the one illustrated in Eq. (9) in that its physical description is not limited to just small amplitude oscillations but covers particle oscillations of any amplitude ranges. Further, Eq. (5) does not depend on quantities like v_{dn} and Ω_v , which terms must be determined experimentally. Instead, Eq. (5) completely describes the dynamics of charged-particle motion solely based on the information obtained from the particle's physical properties (i.e., mass, surface charge density, and dielectric constant, etc.) and the local electric field strength. In the case where the mass of an ionized particle is represented by that of an ionized atom, Eq. (5) describes the dynamics of self-oscillating ionized atom in the DC glow discharges. In the previous work,²⁹ I have discussed that Eq. (5) yields results that qualitatively agree with certain aspects of self-oscillations in the DC glow corona experiments predicted by theories based on the fluid models.^{23,25} If plasma in the DC glow corona experiment is effectively treated as a self-oscillating weakly ionized single superparticle, Eq. (5) provides a satisfactory description of the electrode current oscillations in the DC glow corona. Further discussion on this is provided in the section E of the appendix.

Until now, no single theory was able to successfully explain self-sustained oscillations in both dusty plasmas and DC glow discharges experiments. For years, experimental evidences hinted that these were related phenomena, but without any definitive conclusions. In this respect, Eq. (5) is the first theoretical model to provide such definitive conclusions.

IV. DEVICE APPLICATION

It is well known that oscillating ions generate electric dipole radiation. Such property can be utilized to develop a wideband electromagnetic radiation source in which the frequency of emitted radiation can be tuned by varying the DC bias voltage across the electrodes.^{27,29} According to Zouche and Lefort, the plane-parallel plate electrodes made of nickel-silver composite material, which are separated by a gap of $h = 100$ nm, can support DC bias voltages up to ~ 400 V across the electrodes before an onset of electrical breakdown.⁴³ With improvements in the electrical breakdown characteristics, such device can be engineered to cover both the microwave and the terahertz band of electromagnetic spectrum with high efficiency.

The first experimental evidence that the phenomenon of self-sustained ion oscillations in the DC glow discharges has a potential applications in the development of a wideband electromagnetic radiation source came from McClure in 1963, when he reported an oscillation frequency of $\nu_{osc} \approx 20$ MHz in a low pressure glow discharge tube, which comprised of cylindrical hollow cathode and a very thin coaxial wire anode.⁴⁴ Unfortunately, McClure provided no theoretical model to explain his finding. Such concentric cylinder configuration for the electrodes is a typical apparatus found in many DC glow discharges experiments. Nearly two decades later, in 1980, Alexeff and Dyer shrunk the aforementioned concentric cylinder configuration (filled with air at gas pressure of 0.1 mTorr) to the size of a pen and successfully demonstrated the generation of microwave radiations in the gigahertz frequency ranges.⁴⁵ Their pen sized coaxial configuration was later reported to generate radiation at terahertz frequency of $\nu_{osc} \approx 1$ THz with an output radiation power of $P_{rad} \approx 1.5$ W.^{46,47} In order to explain their observations, Alexeff and Dyer proposed a model which they referred to as the *orbitron theory*.⁴⁵⁻⁴⁷ The basic idea behind the orbitron theory is very simple. The electrons emitted from the inner surface of the outer concentric cylinder (which part represents the cathode in the coaxial configuration) orbit around a thin coaxial wire anode; and, such electron orbital motion generates the detected high frequency electromagnetic radiation. However, various experimental results reported by other groups⁴⁸⁻⁵⁰ contradicted the orbitron model; and, the orbitron theory is no longer considered as the correct description of the physics behind the observations reported by Alexeff and Dyer.

Somewhat similar to the aforementioned pen sized coaxial configuration investigated by Alexeff and Dyer is the microhollow cathode discharges (MHCDs) configuration, which was first introduced by Schoenbach *et al.*¹³ However, unlike the coaxial configuration, where the self-pulsing frequencies of ions typically lie in the gigahertz ranges, the self-pulsing of ions in the DC glow discharges for typical MHCDs configurations lie only in some tens of kilohertz frequency ranges.^{21,51,52} Why? The answer to such discrepancy lies in the differences in the gas pressures applied in two configurations. In the high frequency design by Alexeff and Dyer, the pen sized coaxial device is filled with gas at a very low gas pressure of 0.1 mTorr whereas, in typical MHCDs configura-

tions, the device is maintained at gas pressures on the order of tens (or hundreds) of torrs. For instance, in the MHCDs experiment by Aubert *et al.*,^{51,52} the gas pressure ranged from 40 to 200 Torr. He *et al.*²¹ worked with somewhat lower gas pressure of ~ 1 Torr (i.e., 133 Pa) for their MHCDs experiment, but compared to the gas pressure of 0.1 mTorr used by Alexeff and Dyer in their pen sized coaxial configuration, this is still larger by a factor of ten thousand. Consequently, in the aforementioned MHCDs experiments, the DC glow discharges involve much weaker static electric fields due to larger screening effects. When a gas filled medium is applied with an external static electric field, the polarization process sets in and such screening effect weakens the net electric field strength in the region filled with gas. The degree of such screening process grows with gas pressure. Consequently, in typical MHCDs experiments, where much higher gas pressures are involved, relatively low self-pulsing frequencies are observed as a result of larger screening effects for the applied static electric field. Contrary to this, in the aforementioned pen sized coaxial configuration investigated by Alexeff and Dyer, the externally applied static electric field is only weakly screened due to the fact that the device is maintained at a very low gas pressures. Consequently, the ions in such device can oscillate at very high frequencies.

Besides this screening effect which acts to weaken the externally applied static electric field, the presence of higher gas pressure increases the effective mass of an oscillating superparticle. The superparticle concept has been previously introduced in the discussion of self-oscillations involving a plasma fireball. The dynamics of plasma involves collective motions of its constituent atoms. In the framework of this alternative theory^{27,29} elaborated in this paper, the self-pulsing dynamics in both MHCDs experiments and the pen sized coaxial configuration investigated by Alexeff and Dyer involves the concept of oscillating superparticles. The effective masses of such superparticles have an explicit dependence on gas pressures. In general, the superparticle associated with the higher gas pressure environment has a larger mass than the one associated with the lower gas pressure environment. Consequently, the superparticle in a typical MHCDs experiment has much larger mass than the one in the pen sized coaxial configuration investigated by Alexeff and Dyer. This also explains why self-pulsing frequencies are much lower in MHCDs experiments compared to the device investigated by Alexeff and Dyer.

V. CONCLUDING REMARKS

In summary, the mechanism behind self-sustained oscillations of an ion in the DC glow discharges has been briefly discussed in the framework of interaction between an ion and surface charges that it induces at the bounding electrodes. Such alternative description provides an elegant explanation to the formation of plasma fireballs in the laboratory plasma. It has been found that oscillation frequencies also increase with ion's surface charge density, but at the rate which is significantly slower than it does with electric field strength. Such result supports the conclusions by Fox³ and Bořan *et al.*,³⁶

where they reported of oscillation frequencies being not too dependent on the type of ions used in the discharge. Self-sustained oscillations in the DC glow discharges can be expected to have high thermal stability due to ion's kinetic energies that are much larger than the average room temperature thermal energies. It is well known that self-sustained oscillations in the DC glow discharges occur only in the negative resistance region of the voltage-current characteristic curve. Experimentally, such region is characterized by $V_{th1} \leq V_T \leq V_{th2}$, where V_{th1} and V_{th2} are some threshold voltages. Such observation is quite elegantly explained from the solutions of Eq. (5), where the physical solutions are only found for $V_{th1} \leq V_T \leq V_{th2}$. Presented mechanism also correctly describes the self-sustained oscillations of ions in dusty plasmas. To demonstrate this, Eq. (5) has been applied to correctly predict the frequency of dust particle oscillations in the dusty plasmas experiment by Arnas *et al.*⁴⁰ Such result demonstrates that self-sustained oscillations in dusty plasmas and DC glow discharges involve common physical processes. This is the first theory to successfully explain the self-sustained oscillations phenomena in both dusty plasmas and the DC glow corona physics.

APPENDIX

A. Sheath potential

It is worthwhile to compare the potential energy well of Fig. 2 with the empirical potential well introduced by Tomme *et al.*³⁴ to describe the potential in the plasma sheath. The plasma sheath is an empty space residing between the plasma and the confining electrodes. One such plasma sheath near the anode is illustrated in Fig. 5(a). For the reason that electrons and ions move at different velocities due to the difference in their masses, plasmas are never completely neutral at any instant. Consequently, a plasma confined between DC voltage biased electrodes effectively behaves as if it were a super large charged-particle. For brevity, such "super large charged-particle" shall be simply referred to as a "plasma ball" throughout the discussion here. In fact, the single ionized nanoparticle case illustrated in Fig. 5(b) is the limit in which the plasma in Fig. 5(a) reduces down to contain just one ionized nanoparticle. That said, just as single ionized nanoparticle self-oscillates when confined by DC voltage biased electrodes, the plasma ball also self-oscillates between the anode and cathode electrodes.⁹ However, due to its large mass, the plasma ball oscillates at much lower frequencies compared to the nanoparticle counterparts. For instance, assuming the gap h between the plate electrodes is in the order of sub-millimeters or so in Fig. 5(a), the macroscopic plasma confined between such electrodes can contain very large number, i.e., say, millions or more, of ionized nanoparticles or atoms depending on the gas pressure. In general, for the study of self-sustained oscillations, the plasma ball illustrated in Fig. 5(a) can be effectively modeled using an ionized superparticle, where the terminology superparticle refers to a particle which is extremely large and enormously heavier compared to the

ionized nanoparticle (or atom) illustrated in Fig. 5(b). In such model, the potential in the plasma sheath is represented by the one presented in this article. It is quite remarkable that the sheath potential introduced empirically by Tomme *et al.* closely resembles the potential described in this work.

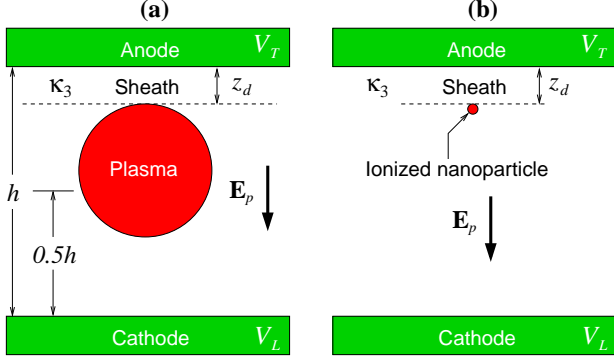


Figure 5: (Color online) (a) Illustration of the plasma and the sheath. The plasma ball effectively behaves as one very large charged superparticle. In the illustration, the plasma has been deliberately drawn as a sphere to emphasize a plasma ball. In reality, however, the plasma can be in any shape depending on the geometry of confining electrodes. (b) The single ionized particle configuration considered in this article. In (a) and (b), only the sheath near the anode is shown for illustration.

B. Parameters in experiment by Arnas *et al.*

Arnas *et al.*⁴⁰ reported that a dust particle made of hollow glass microsphere of radius $r \approx 32 \mu\text{m}$ with mass density $\rho_m \approx 110 \text{kg/m}^3$ and carrying a total charge of $Q \approx -4.3 \times 10^5 q_e$, where $q_e = 1.602 \times 10^{-19} \text{C}$, self-oscillates at frequency of $\nu_{\text{osc}} \approx 17 \text{Hz}$ inside the plasma sheath. The inner environment of the plasma sheath, in many respects, is similar to the environment in an empty space between the DC voltage biased plane-parallel conductors. In that regard, the undamped self-sustained oscillations of charged glass microsphere in the experiment by Arnas *et al.* should be theoretically describable using the model presented in this article, where a core-shell structured charged particle is confined between the DC voltage biased plane-parallel conductors. The glass microsphere used by Arnas *et al.* is not core-shell structured, of course. Such dielectric particle is obtained in the limit the radius of conductive core portion of the core-shell structured particle goes to zero, i.e., $a = 0$. Consequently, σ_1 also vanishes in that limit. That said, the glass microsphere of radius $b = 32 \mu\text{m}$ with mass density $\rho_m \approx 110 \text{kg/m}^3$ has total mass of $m = (4/3) \pi b^3 \rho_m$ or $m \approx 1.51 \times 10^{-11} \text{kg}$. Although Arnas *et al.* specifically uses the word “hollow glass microsphere” in their report, they do not provide any physical details of the particle other than its outer radius. Thus, in the aforementioned calculation of the particle’s mass, I have assumed a solid glass microsphere. The glass microsphere carries a total charge of $Q \approx -4.3 \times 10^5 q_e$, where $q_e = 1.602 \times 10^{-19} \text{C}$. The surface charge density at the radius $r = b$ is hence given

by $\sigma_2 = Q / (4\pi b^2)$ or $\sigma_2 = -5.35 \mu\text{C/m}^2$. Arnas *et al.* does not provide any information regarding the dielectric constant κ_2 for their glass microsphere. Therefore, $\kappa_2 = 6.5$ has been chosen for the dielectric constant of glass microsphere, which value is typical of glass microspheres. For convenience, it shall be assumed that the medium in which the glass microsphere oscillates is a vacuum, i.e., $\kappa_3 = 1$. The parameters in the experiment by Arnas *et al.* is summarized here for reference:

$$\begin{cases} \kappa_2 = 6.5, \kappa_3 = 1, h = 5 \text{ mm}, E_p = 5.15 \text{ kV/m}, \\ \sigma_1 = 0 \text{ C/m}^2, \sigma_2 = -5.35 \mu\text{C/m}^2, \\ m \approx 15.1 \text{ ng}, a = 0 \text{ m}, b = 32 \mu\text{m}, \end{cases} \quad (10)$$

where the mass is in nanograms, i.e., $m \approx 1.51 \times 10^{-11} \text{kg} = 15.1 \text{ ng}$. The initial conditions,

$$z_d(0) = 4.4 \text{ mm} \quad \text{and} \quad \frac{dz_d(0)}{dt} = 0 \frac{\text{mm}}{\text{s}}, \quad (11)$$

have been chosen purely out of convenience. With Eqs. (10) and (11), the equation of motion defined in Eq. (5) can be solved numerically via Runge-Kutta method to obtain the results illustrated in Fig. 4. One can readily verify that the theory agrees with the experiment.⁴⁰

C. Comparison to the potential energy of negatively charged glass microsphere measured by Arnas *et al.*

According to the model elaborated here,²⁹ the positively charged particle confined between a DC voltage biased plane-parallel conductors results in the formation of potential energy well in vicinity of the anode whereas a negatively charged particle results in the formation of potential energy well in vicinity of the cathode. Arnas *et al.*³⁵ have experimentally verified such potential energy well for the case of negatively charged particle in the plasma sheath near the cathode. As explained previously, the problem of charged particle inside the plasma sheath can be effectively modeled by a charged particle confined by the DC voltage biased plane-parallel conductors. The potential energy function $U(z_d)$ of Eq. (4) has been plotted for the following parameter values:

$$\begin{cases} \kappa_2 = 6.5, \kappa_3 = 1, h = 5 \text{ mm}, E_p = 3.15 \text{ kV/m}, \\ \sigma_1 = 0 \text{ C/m}^2, \sigma_2 = -5.795 \mu\text{C/m}^2, \\ m \approx 4.91 \times 10^{-12} \text{ kg}, a = 0 \text{ m}, b = 22 \mu\text{m}. \end{cases} \quad (12)$$

The result is shown in Fig. 6, where it shows the formation of potential energy well in vicinity of the cathode. One notices that the order of magnitude for the potential energy well is comparable to the experiment by Arnas *et al.* The minor discrepancies in the potential energy well of Fig. 6 and the one measured by Arnas *et al.*³⁵ can be attributed to the fact that the electric field is not constant in the plasma sheath whereas, between the DC voltage biased plane-parallel conductors, electric field is a constant.

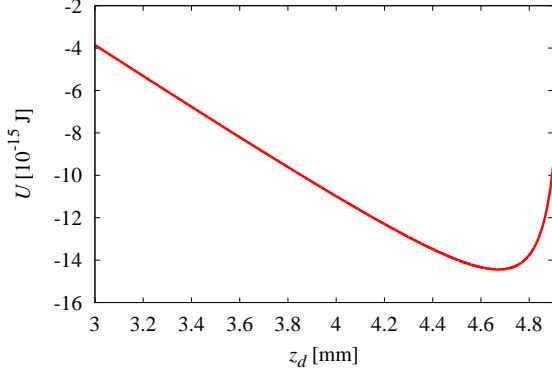


Figure 6: The potential energy of Eq. (4) is plotted for parameter values defined in Eq. (12). In the plot, the anode is located at $z_d = 0$ mm and the cathode is located at $z_d = 5$ mm. This result should be compared with the potential energy measured by Arnas *et al.*³⁵ in their dusty plasmas experiment. One can verify that two results are remarkably similar in potential energy profile as well as in the order of magnitudes.

D. Physical and unphysical oscillatory solutions

The oscillatory solutions obtained for $E_p \lesssim 0.1$ GV/m and $E_p \gtrsim 4.9$ GV/m are unphysical in Fig. 3(d). To demonstrate this, Eq. (5) is numerically solved and plotted for $E_p \lesssim 0.1$ GV/m and $E_p \gtrsim 4.9$ GV/m using the following initial conditions and parameter values:

$$\begin{cases} \kappa_2 = \infty, \kappa_3 = 1, h = 100 \text{ nm}, V_L = 0 \text{ V}, \\ \sigma_1 \approx 3.19 \text{ C/m}^2, \sigma_2 = 0 \text{ C/m}^2, \\ m \approx 8.95 \times 10^{-24} \text{ kg}, b = a = 1 \text{ nm}, \\ z_d(0) = 0.5 \text{ nm}, \dot{z}_d(0) = 0 \text{ nm/s}, \dot{z}_d \equiv dz_d/dt. \end{cases} \quad (13)$$

To show that $E_p \lesssim 0.1$ GV/m yields unphysical solutions, $z_d(t)$ is plotted for $E_p = 0.1$ GV/m and $E_p = 0.09$ GV/m. The results are shown in Fig. 7, where the surface of anode is at $z_d = 0$ nm, the surface of cathode is at $z_d = 100$ nm, and the midway between the plates is at $z_d = 50$ nm. It can be clearly seen that for $E_p = 0.09$ GV/m, positively ionized particle periodically crosses the midway between the two electrodes. Such case is unphysical because, for positively ionized particles, oscillations can only exist for $z_d < h/2 - b$.²⁷ Now, it can be verified that any E_p less than $E_p = 0.09$ GV/m yields such unphysical solutions.

To show that $E_p \gtrsim 4.9$ GV/m yields unphysical solutions, $z_d(t)$ is plotted for $E_p = 4.9$ GV/m and $E_p = 5.0$ GV/m. The results are shown in Fig. 8(a), where the plot has been enlarged for a view near $z_d = 0$ pm in Fig. 8(b). It can be clearly seen that for $E_p = 5.0$ GV/m, positively ionized particle periodically penetrates into the surface of anode, which is unphysical. Now, it can be verified that any E_p larger than $E_p = 5.0$ GV/m yields such unphysical solutions.

For the initial conditions and parameter values defined in Eq. (13), physical solutions for the oscillatory motion of positively ionized particle are only found for E_p satisfying the condition given by $0.1 \text{ GV/m} \lesssim E_p \lesssim 4.9 \text{ GV/m}$, where the

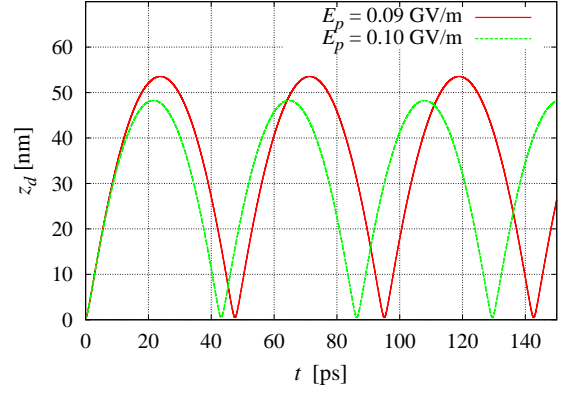


Figure 7: (Color online) Plot of $z_d(t)$ for $E_p = 0.1$ GV/m and $E_p = 0.09$ GV/m. The surface of anode is at $z_d = 0$ nm, the surface of cathode is at $z_d = 100$ nm, and the midway between the two electrodes is at $z_d = 50$ nm.

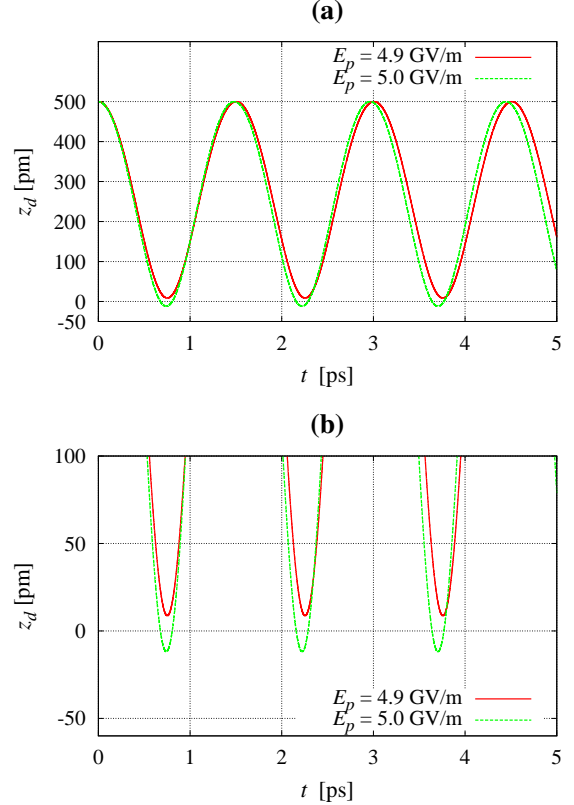


Figure 8: (Color online) (a) Plot of $z_d(t)$ for $E_p = 4.9$ GV/m and $E_p = 5.0$ GV/m. (b) The plot in (a) has been enlarged for a view near $z_d = 0$ pm. The surface of anode is at $z_d = 0$ pm.

upper and lower bounds of E_p are rough estimates based on the grounds of the discussed physicality. This result explains why oscillations suddenly appear at certain “initial” threshold DC bias voltage and disappear suddenly when bias voltage goes beyond certain larger “final” threshold voltage in experiments.

E. Weakly ionized particle confined between anode and cathode plates separated by gap of $h = 1$ mm

The oscillation frequency plot of Fig. 3(d) has been obtained for an highly ionized particle which is confined between two plate electrodes with very small separation gap of $h = 100$ nm. Here, the same calculation is done for a weakly ionized particle confined between plate electrodes with microscopically very large separation gap of $h = 1$ mm. According to Chen *et al.*,³² a spherical argon cluster of radius $r = a = 4.7$ nm contains roughly ~ 9600 argon atoms at backing pressure of 50 bars. Since the particle is assumed to be weakly ionized, I shall assume that $N = 20$ electrons are removed from it. This corresponds to surface charge density of $\sigma_1 = Nq_e / (4\pi a^2)$ or $\sigma_1 \approx 1.1543 \times 10^{-2} \text{ C/m}^2$, where $q_e = 1.602 \times 10^{-19} \text{ C}$ is the fundamental charge unit. Neglecting the masses of missing N electrons, the particle has a total mass of $m \approx 6.365 \times 10^{-22} \text{ kg}$. For the calculation of particle's mass, it has been assumed that single argon atom has mass of $6.63 \times 10^{-26} \text{ kg}$. That said, the following initial conditions and parameter values are used for the calculation of particle's oscillation frequency as function of electric field strength:

$$\begin{cases} \kappa_2 = \infty, \kappa_3 = 1, h = 1 \text{ mm}, V_L = 0 \text{ V}, \\ \sigma_1 \approx 11.543 \text{ mC/m}^2, \sigma_2 = 0 \text{ C/m}^2, \\ m \approx 6.365 \times 10^{-22} \text{ kg}, b = a = 4.7 \text{ nm}, \\ z_d(0) = 10 \mu\text{m}, \dot{z}_d(0) = 0 \mu\text{m/s}, \dot{z}_d \equiv dz_d/dt. \end{cases} \quad (14)$$

Using these, the equation of motion defined in Eq. (5) is solved numerically via Runge-Kutta method for the oscillation frequency as function of electric field strength; and, the result is shown in Fig. 9.

This result should be compared with the one provided by Akishev *et al.*,²⁵ where they have plotted both experimental and calculated period T_{osc} of self-sustained oscillations against the average corona current at different pressures of nitrogen. Fox³ and Bořan *et al.*³⁶ have shown that oscillation frequencies are not very dependent on the type of ionized particles used in the discharge. That said, the result obtained by Akishev *et al.* for nitrogen gas can be compared with the calculation done here for ionized spherical argon cluster. Recalling that $\nu_{\text{osc}} = 1/T_{\text{osc}}$ and the average corona current in the electrode increases with electric field strength, it can be readily convinced that the profile of result shown in Fig. 9 is consistent with the result obtained by Akishev *et al.*

Although the profile of oscillation frequency dependence on electric field strength (or corona current in the electrode) is comparable in both results, the measurement by Akishev *et al.* shows much lower oscillation frequencies for given range of electric field strengths. Why? Such discrepancy arises from the fact that in the experiment by Akishev *et al.*, the self-oscillating object is a charged plasma ball, i.e., charged superparticle, whereas in the calculation of Fig. 9, the self-oscillating object is a charged nanoparticle. As already discussed in section A, a macroscopic plasma ball contains very large number of ionized nanoparticles (or atoms) depending on the gas pressure. This makes macroscopic plasma ball ef-

fectively a single charged superparticle with very large mass.

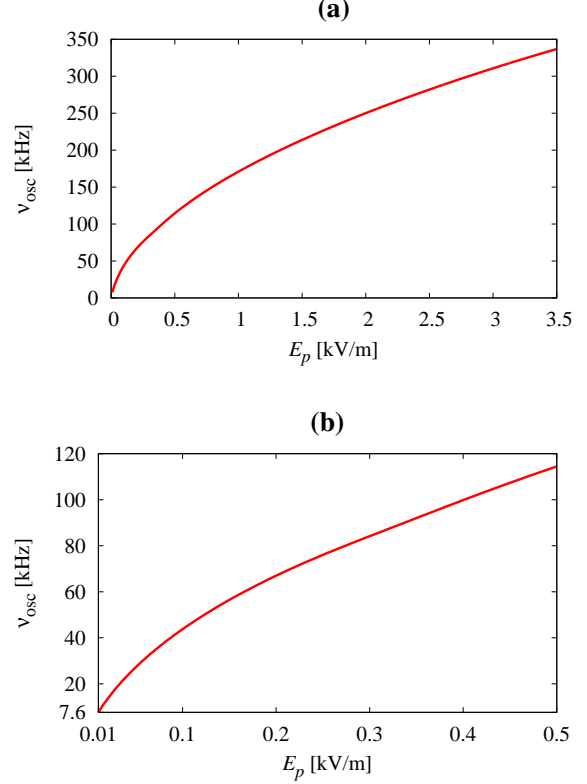


Figure 9: (a) The frequency of oscillations is plotted against electric field strength for a weakly ionized particle with initial conditions and parameters values defined in Eq. (14). (b) The plot in (a) is enlarged near zero. Unlike the case illustrated in Fig. 3(d), where ionized particle is confined between electrodes with very small gap, the result here involves very large number of discretized time steps for the Runge-Kutta routine. For that reason, the oscillation frequency has been plotted from $E_p = 0.01 \text{ kV/m}$ to $E_p = 3.5 \text{ kV/m}$ in (a). The threshold electric field strengths, i.e., $E_{p,\text{th1}}$ and $E_{p,\text{th2}}$, are not shown in the figure.

It has been illustrated in Fig. 4 that an ionized particle with smaller mass requires weaker electric field strength compared to the one with larger mass to oscillate at the same frequency. Mathematically, such characteristic arises from the fact that Eq. (5) has mass dependence in the denominator. Consequently, the plasma ball in the experiment by Akishev *et al.*, which effectively behaves as a single charged superparticle, oscillates at much lower frequencies for the given range of electric field strengths compared to the configuration used in Fig. 9, where the mass of an ionized particle is much smaller than the effective mass of a plasma ball. In principle, once the mass and the effective total charge information of the plasma ball, i.e., superparticle, are provided, the oscillation frequency dependence on corona current in the electrode (or electric field strength) measured by Akishev *et al.* can be reproduced by the presented theory.

-
- * Electronic address: sungnae.cho@samsung.com
- ¹ L. Pardue and J. Webb, Phys. Rev. **32**, 946 (1928).
 - ² G. Fox, Phys. Rev. **35**, 1066 (1930).
 - ³ G. Fox, Phys. Rev. **37**, 815 (1931).
 - ⁴ T. Donahue and G. Dieke, Phys. Rev. **81**, 248 (1951).
 - ⁵ L. Colli, U. Facchini, E. Gatti, and A. Persano, J. Appl. Phys. **25**, 429 (1954).
 - ⁶ A. Pilon, Phys. Rev. **107**, 25 (1957).
 - ⁷ K. Ogawa, J. Phys. Soc. Jpn. **14**, 1746-1751 (1959).
 - ⁸ M. Goldman, A. Goldman, and R. Sigmond, Pure & Appl. Chem. **57**(9), 1353-1362 (1985).
 - ⁹ A. Piel, H. Klostermann, A. Rohde, N. Jelić, and R. Schrittwieser, Phys. Lett. A **216**, 296 (1996).
 - ¹⁰ Z. Petrović, I. Stefanović, S. Vrhovac, and J. Živković, J. Phys. IV France **7**, C4-341 (1997).
 - ¹¹ R. Sigmond, J. Phys. IV France **7**, C4-383 (1997).
 - ¹² Z. Petrović and A. Phelps, Phys. Rev. E. **56**, 5920 (1997).
 - ¹³ K. Schoenbach, A. El-Habachi, W. Shi, and M. Ciocca, Plasma Sources Sci. Technol. **6**, 468 (1997).
 - ¹⁴ E. Lozneau, V. Popescu, and M. Sanduloviciu, J. Appl. Phys. **92**, 1195 (2002).
 - ¹⁵ M. Makarov, Y. Loumani, and A. Kozyrev, J. Appl. Phys. **100**, 033301 (2006).
 - ¹⁶ R. Stenzel, J. Gruenwald, C. Ionita, and R. Schrittwieser, Plasma Sources Sci. Technol. **20**, 045017 (2011).
 - ¹⁷ T. Kuschel, B. Niemann, I. Stefanović, M. Böke, N. Škoro, D. Marić, Z. Petrović, and J. Winter, Plasma Sources Sci. Technol. **20**, 065001 (2011).
 - ¹⁸ A. Phelps, Z. Petrović, and B. Jelenković, Phys. Rev. E. **47**, 2825 (1993).
 - ¹⁹ D. Hsu and D. Graves, J. Phys. D: Appl. Phys. **36**, 2898 (2003).
 - ²⁰ P. Chabert, C. Lazzaroni, and A. Rousseau, J. Appl. Phys. **108**, 113307 (2010).
 - ²¹ S. He, J. Ouyang, F. He, and H. Jia, Phys. Plasmas **19**, 023504 (2012).
 - ²² I. Pérès and L. Pitchford, J. Appl. Phys. **78**, 774 (1995).
 - ²³ R. Morrow, J. Phys. D: Appl. Phys. **30**, 3099 (1997).
 - ²⁴ Z. Donkó, J. Phys. D: Appl. Phys. **32**, 1657 (1999).
 - ²⁵ Yu. Akishev, M. Grushin, A. Deryugin, A. Napartovich, M. Pan'kin, and N. Trushkin, J. Phys. D: Appl. Phys. **32**, 2399 (1999).
 - ²⁶ N. Allen, M. Abdel-Salam, M. Boutlendj, I. Cotton, and B. Tan, IET Sci. Meas. Technol. **1**(2), 103 (2007).
 - ²⁷ S. Cho, Phys. Plasmas **19**, 033506 (2012).
 - ²⁸ B. MacGibbon, G. Garino, M. Lucas, A. Nathan, G. Feldman, and B. Dolbilkin, Phys. Rev. C **52**, 2097 (1995).
 - ²⁹ S. Cho, Phys. Plasmas **19**, 072113 (2012).
 - ³⁰ E. Becker, K. Bier, and W. Henkes, Z. Phys. **146**, 133 (1956).
 - ³¹ L. Bartell, B. Raoult, and G. Torchet, J. Chem. Phys. **66**, 5387 (1977).
 - ³² G. Chen, B. Kim, B. Ahn, and D. Kim, J. Appl. Phys. **106**, 053507 (2009).
 - ³³ R. Stenzel, C. Ionita, and R. Schrittwieser, Plasma Sources Sci. Technol. **17**, 035006 (2008).
 - ³⁴ E. Tomme, B. Annaratone, and J. Allen, Plasma Sources Sci. Technol. **9**, 87 (2000).
 - ³⁵ C. Arnas, M. Mikikian, G. Bachet, and F. Doveil, Phys. Plasmas **7**, 4418 (2000).
 - ³⁶ Dj. Bošan, V. Zlatić, and B. Mijović, J. Phys. D: Appl. Phys. **21**, 1462 (1988).
 - ³⁷ C. Lotze, M. Corso, K. Franke, F. von Oppen, and J. Pascual, Science **338**, 779 (2012).
 - ³⁸ J. Gupta, C. Lutz, A. Heinrich, and D. Eigler, Phys. Rev. B **71**, 115416 (2005).
 - ³⁹ A. Senftleben, O. Al-Hagan, T. Pflüger, X. Ren, D. Madison, A. Dorn, and J. Ullrich, J. Chem. Phys. **133**, 044302 (2010).
 - ⁴⁰ C. Arnas, M. Mikikian, and F. Doveil, Phys. Rev. E. **60**, 7420 (1999).
 - ⁴¹ V. Fortov, A. Khrapak, S. Khrapak, V. Molotkov, and O. Petrov, Phys. Usp. **47**(5), 447 (2004).
 - ⁴² A. Melzer, T. Trottenberg, and A. Piel, Phys. Lett. A **191**, 301 (1994).
 - ⁴³ N. Zouache and A. Lefort, IEEE Trans. Dielectr. Electr. Insul. **4**(4), 358 (1997).
 - ⁴⁴ G. McClure, Appl. Phys. Lett. **2**, 233 (1963).
 - ⁴⁵ I. Alexeff and F. Dyer, Phys. Rev. Lett. **45**, 351 (1980).
 - ⁴⁶ I. Alexeff, F. Dyer, and W. Nakoneczny, Int. J. Infrared Millim. Waves **6**, 481 (1985).
 - ⁴⁷ I. Alexeff, F. Dyer, and M. Radar, Nucl. Inst. Meth. Phys. Res. A **285**, 228 (1989).
 - ⁴⁸ R. Schumacher and R. Harvey, Bull. Am. Phys. Soc. **29**, 1179 (1984).
 - ⁴⁹ J. Felsteiner, A. Rosenberg, D. Arbel, and J. Politch, Int. J. Infrared Millim. Waves **8**, 479 (1987).
 - ⁵⁰ R. Stenzel, Phys. Rev. Lett. **60**, 704 (1988).
 - ⁵¹ A. Rousseau and X. Aubert, J. Phys. D: Appl. Phys. **39**, 1619 (2006).
 - ⁵² X. Aubert, G. Bauville, J. Guillon, B. Lacour, V. Puech, and A. Rousseau, Plasma Sources Sci. Technol. **16**, 23 (2007).